

Electronic Supplementary Information

Synergistic design of N, O codoped honeycomb carbon electrode and ionogel electrolyte enabling all-solid-state supercapacitor with an ultrahigh energy density

Ziyang Song,^a Liangchun Li,^a Dazhang Zhu,^a Ling Miao,^a Hui Duan,^a Zhiwei Wang,^b Wei Xiong,^c Yaokang Lv,^d Mingxian Liu,^{*ab} and Lihua Gan^{*a}

^a Shanghai Key Lab of Chemical Assessment and Sustainability, School of Chemical Science and Engineering, Tongji University, Shanghai 200092, P. R. China.

^b State Key Laboratory of Pollution Control and Resources Reuse, Shanghai Institute of Pollution Control and Ecological Security, School of Environmental Science and Engineering, Tongji University, Shanghai 200092, P. R. China.

^c Key Laboratory for Green Chemical Process of Ministry of Education, School of Chemistry and Environmental Engineering, Wuhan Institute of Technology, Wuhan 430073, P. R. China.

^d College of Chemical Engineering, Zhejiang University of Technology, Hangzhou 310014, P. R. China.

*Corresponding Authors

E-mail: liumx@tongji.edu.cn, ganlh@tongji.edu.cn

Table S1 Synthesis parameters of HPC^a.

| Samples | Effect factors | Water (mL) | Temperature (°C) |
|---------|----------------|------------|------------------|
| HPC-1 | | 120 | 700 |
| HPC-2 | Solvent | 180 | 700 |
| HPC-3 | | 240 | 700 |
| HPC-4 | | 180 | 600 |
| HPC-5 | Temperature | 180 | 800 |
| HPC-6 | | 180 | 900 |

^aTemperature: activation temperature; S_{BET} : specific surface area; N, O: nitrogen and oxygen contents of HPC; C_m : gravimetric specific capacitance of HPC electrodes tested in three-electrode system using KOH electrolyte.

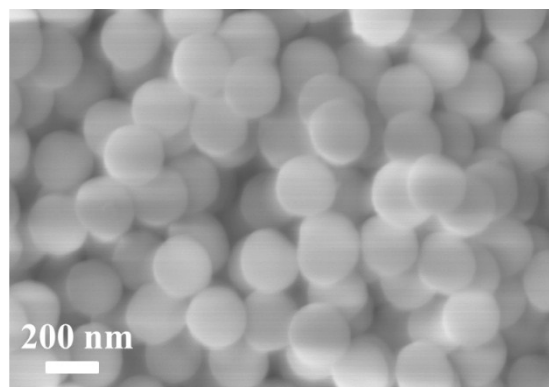


Fig. S1 SEM image of SiO_2 .

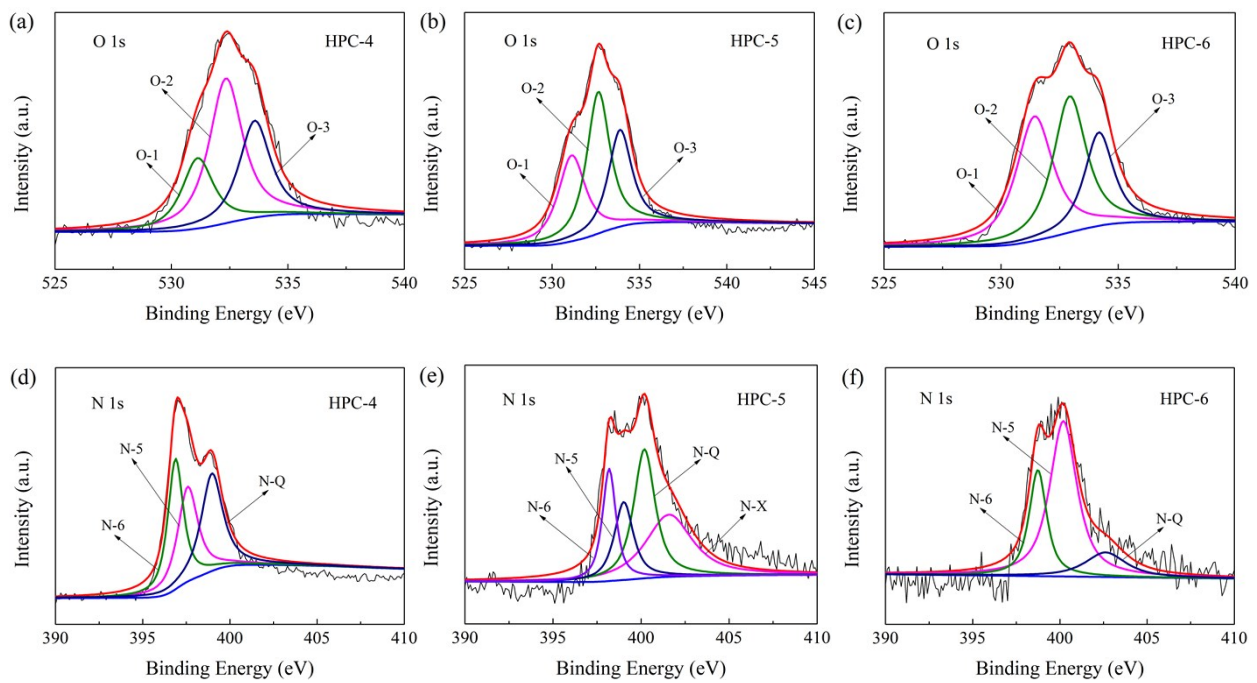


Fig. S2 High-resolution XPS spectra of O 1s (a–c) and N 1s (d–f) for HPC-4 (a, d), HPC-5 (b, e) and HPC-6 (c, f) prepared at different activation temperatures.

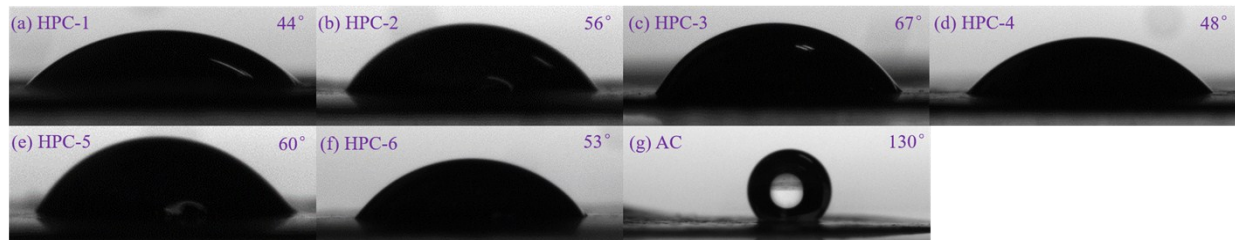


Fig. S3 The water contact angles of HPC (a–f) and commercial activated carbon (AC, g).

Table S2 Elemental compositions (wt.%) of HPC and relative contents of N and O species to N 1s and O 1s in HPC.

| Samples | N | O | N-6 (%) | N-5 (%) | N-Q (%) | O-1 (%) | O-2 (%) | O-3 (%) |
|---------|-------|-------|----------|----------|----------|----------|----------|----------|
| | | | 398.1 eV | 399.8 eV | 401.3 eV | 530.5 eV | 531.8 eV | 533.7 eV |
| HPC-1 | 8.72 | 15.73 | 31.18 | 34.53 | 34.29 | 29.49 | 42.78 | 27.73 |
| HPC-2 | 6.90 | 10.17 | 24.94 | 59.68 | 15.39 | 36.56 | 38.29 | 25.15 |
| HPC-3 | 6.51 | 10.75 | 26.37 | 55.74 | 17.89 | 28.48 | 48.44 | 23.08 |
| HPC-4 | 10.23 | 14.04 | 33.45 | 31.86 | 34.69 | 22.13 | 48.01 | 29.86 |
| HPC-5 | 5.10 | 10.51 | 21.95 | 32.55 | 45.50 | 30.07 | 41.42 | 28.51 |
| HPC-6 | 2.39 | 12.64 | 26.18 | 59.71 | 14.11 | 38.97 | 38.13 | 22.90 |

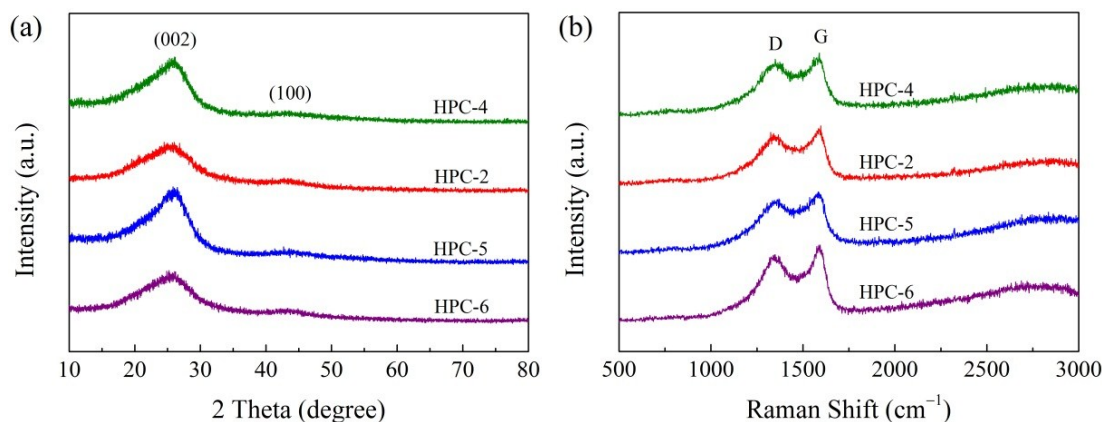


Fig. S4 XRD patterns (a) and Raman spectra (b) of HPC.

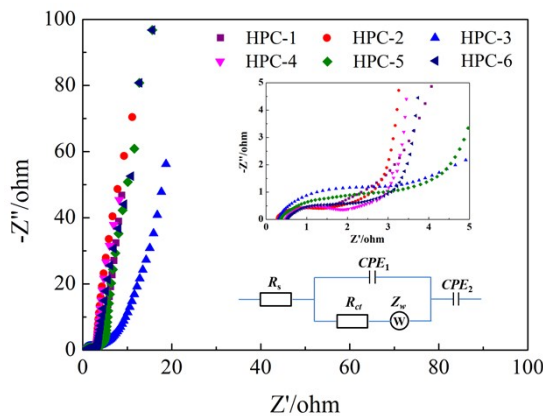


Fig. S5 Nyquist plots of HPC electrodes.

Table S3 Components of the equivalent circuit fitted for the impedance spectra.

| Samples | R_s (Ω) | R_{ct} (Ω) | Z_w (Ω) |
|---------|--------------------|-----------------------|--------------------|
| HPC-1 | 0.29 | 1.12 | 0.58 |
| HPC-2 | 0.27 | 0.98 | 0.56 |
| HPC-3 | 0.32 | 3.46 | 0.84 |
| HPC-4 | 0.48 | 1.34 | 0.77 |
| HPC-5 | 0.37 | 3.07 | 0.73 |
| HPC-6 | 0.52 | 1.80 | 0.61 |

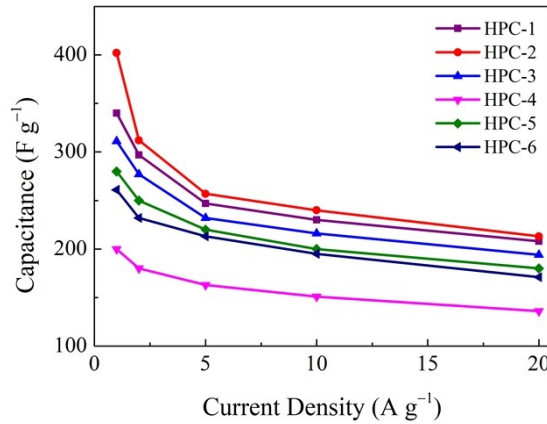


Fig. S6 Specific capacitances of HPC electrodes at different current densities.

Table S4 Comparison of surface areas (S_{BET}), heteroatom contents, specific capacitances (C_m) under different current densities (I_m) of reported heteroatom-doped carbon electrodes tested in a three-electrode system using 6 M KOH in the literatures.

| Materials | S_{BET} ($\text{m}^2 \text{ g}^{-1}$) | N/O (wt.%) | C_m (F g^{-1}) | I_m (A g^{-1}) | Ref. |
|------------------------------------|---|---------------|--------------------------------|--------------------------------|-----------|
| N-doped 3D graphene networks | 583 | 15.8/6.93 | 380 | 0.6 | 1 |
| N-doped graphene | – | 4.2/14.5 | 312 | 0.1 | 2 |
| Graphene nanocomposite | 2416 | 2/– | 176 | 0.5 | 3 |
| 3D binary-heteroatom doped carbon | 1532 | 14.5/– | 341 | 0.1 | 4 |
| Porous carbon | 3122 | –/9.84 | 327 | 0.5 | 5 |
| 3D porous carbon | 1874 | 5.11/– | 404 | 0.1 | 6 |
| 2D carbons | 594 | 4.04/– | 233 | 1 | 7 |
| N-doped graphdiyne | 679 | 3.67/– | 250 | 0.2 | 8 |
| N-doped carbon nanofibers | 418 | 7.85/5.35 | 307 | 1 | 9 |
| Ultrathin porous carbon nanosheets | 1192 | –/10.6 | 233 | 1 | 10 |
| N-doped carbon nanosheets | 2494 | 4.7/– | 242 | 0.1 | 11 |
| N-doped carbons | 329 | 13.44/– | 374 | 0.1 | 12 |
| HPC-2 | 2379 | 6.90/10.17 | 533 | 0.5 | This work |
| | | | 402 | 1 | |

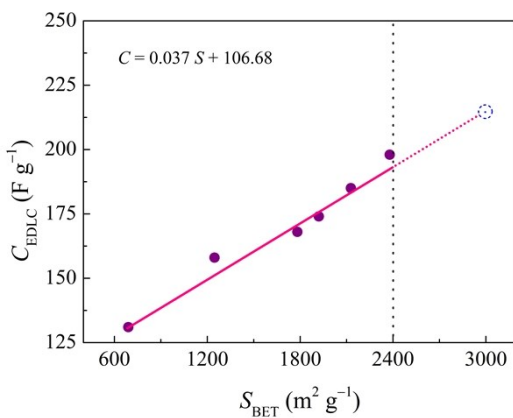


Fig. S7 The relationship between surface areas and C_{EDLC} of HPC electrodes.

References

- 1 W. Zhang, C. Xu, C. Ma, G. Li, Y. Wang, K. Zhang, F. Li, C. Liu, H.M. Cheng, Y. Du, N. Tang, W. Ren, *Adv. Mater.*, 2017, **29**, 1701677.
- 2 K. Wang, M. Xu, Y. Gu, Z. Gu, J. Liu, Q.H. Fan, *Nano Energy*, 2017, **31**, 486–494.
- 3 L. Feng, K. Wang, X. Zhang, X. Sun, C. Li, X. Ge, Y. Ma, *Adv. Funct. Mater.*, 2018, **28**, 1704463.
- 4 Y. Liu, X. Qiu, X. Liu, Y. Liu, L.-Z. Fan, *J. Mater. Chem. A*, 2018, **6**, 8750–8756.
- 5 J. Yang, H. Wu, M. Zhu, W. Ren, Y. Lin, H. Chen, F. Pan, *Nano Energy*, 2017, **33**, 453–461.
- 6 Y. Liu, Z. Xiao, Y. Liu, L.-Z. Fan, *J. Mater. Chem., A* 2018, **6**, 160–166.
- 7 W. Liu, M. Ulaganathan, I. Abdelwahab, X. Luo, Z. Chen, S.J. Rong Tan, X. Wang, Y. Liu, D. Geng, Y. Bao, J. Chen, K.P. Loh, *ACS Nano*, 2018, **12**, 852–860.
- 8 H. Shang, Z. Zuo, H. Zheng, K. Li, Z. Tu, Y. Yi, H. Liu, Y. Li, Y. Li, *Nano Energy*, 2018, **44**, 144–154.
- 9 L.-F. Chen, Y. Lu, L. Yu, X. Lou, *Energy Environ. Sci.*, 2017, **10**, 1777–1783.
- 10 K. Jayaramulu, D.P. Dubal, B. Nagar, V. Ranc, O. Tomanec, M. Petr, K.K.R. Datta, R. Zboril, P. Gomez-Romero, R.A. Fischer, *Adv. Mater.*, 2018, **30**, 1705789.
- 11 J. Hou, C. Cao, F. Idrees, X. Ma, *ACS Nano*, 2015, **9**, 2556–2564.
- 12 J.-S.M. Lee, M.E. Briggs, C.-C. Hu, A.I. Cooper, *Nano Energy*, 2018, **46**, 277–289.